Published in final edited form as:
Vis Neurosci. 2005 ; 22(6): 825–838.

Gycine and GABA interact to regulate the nitric oxide/cGMP signaling pathway in the turtle retina

DOU YU and **WILLIAM D. ELDRED**
Boston University, Program in Neuroscience, Boston, Massachusetts

Abstract

Nitric oxide (NO) is a free radical that is important in retinal signal transduction and cyclic guanosine monophosphate (cGMP) is a critical downstream messenger of NO. The NO/cGMP signaling pathway has been shown to modulate neurotransmitter release and gap junction coupling in horizontal cells and amacrine cells, and increase the gain of the light response in photoreceptors. However, many of the mechanisms controlling the production of NO and cGMP remain unclear. Previous studies have shown activation of NO/cGMP production in response to stimulation with N-methyl-d-aspartate (NMDA) or nicotine, and the differential modulation of cGMP production by $GABA_A$ and $GABA_C$ receptors ($GABA_A$Rs and $GABA_C$Rs). This study used cGMP immunocytochemistry and NO imaging to investigate how the inhibitory GABAergic and glycinergic systems modulate the production of NO and cGMP. Our data show that blocking glycine receptors (GLYR) with strychnine (STRY) produced moderate increases in cGMP-like immunoreactivity (cGMP-LI) in select types of amacrine and bipolar cells, and strong increases in NO-induced fluorescence (NO-IF). TPMPA, a selective $GABA_C$R antagonist, greatly reduced the increases in cGMP-LI stimulated by STRY, but did not influence the increase in NO-IF stimulated by STRY. Bicuculline (BIC), a $GABA_A$R antagonist, however, enhanced the increases in both the cGMP-LI and NO-IF stimulated by STRY. CNQX, a selective antagonist for α-Amino-3-hydroxy-5-methyl-4-isoxazolepropionic acid hydrobromide/kainic acid (AMPA/KA) receptors, eliminated both the increases in cGMP-LI and NO-IF stimulated by STRY, while MK801, a selective antagonist for NMDA receptors, slightly increased the cGMP-LI and slightly decreased the NO-IF stimulated by STRY. Finally, double labeling of NO-stimulated cGMP and either GLY or GABA indicated that cGMP predominantly colocalized with GLY. Taken together, these findings support the hypothesis that GLY and GABA interact in the regulation of the NO/cGMP signaling pathway, where GLY primarily inhibits NO production and GABA has a greater effect on cGMP production. Such interacting inhibitory pathways could shape the course of signal transduction of the NO/cGMP pathway under different physiological situations.

Keywords

Nitric oxide; cGMP; GABA; Glycine; Turtle; Retina

Introduction

Nitric oxide (NO) functions as a neurotransmitter or neuromodulator in the brain and retina (reviews: Eldred, 2000; Prast & Philippu, 2001). In the retina, NO is associated with the modulation of light responses and neurotransmitter release (Kurenni et al., 1995; Ientile et al., 1997; Savchenko et al., 1997). Cyclic guano-sine monophosphate (cGMP) is an important second messenger in the NO/cGMP signaling pathway, which regulates neurotransmission and

Address correspondence and reprint requests to: William D. Eldred, Boston University, Department of Biology, 5 Cummington Street, Boston, MA 02215, USA. E-mail: eldred@bu.edu.

retinal signal processing in specific cell types such as uncoupling of gap junctions in horizontal cells and amacrine cells (DeVries & Schwartz, 1989; Miyachi et al., 1990; Mills & Massey, 1995), and increasing the gain of light responses in photoreceptors (Savchenko et al., 1997) and bipolar cells (Shiells & Falk, 1992). However, NO has also been recently shown to modulate neurotransmission in the retina independently from cGMP (Ohkuma et al., 1996 a,b; Yu & Eldred, 2005). The largely separate populations of cells that produce either NO or cGMP (Blute et al., 1997, 1998) can potentially activate different signal-transduction pathways under different physiological situations. Previous studies have shown that the excitatory glutamatergic (Blute et al., 1999) and cholinergic (Blute et al., 2003) synaptic pathways, and the inhibitory gamma-amino-n-butyric acid (GABA)-mediated synaptic pathways (Yu & Eldred, 2003) can modulate the production of cGMP. Activation of glutamate (GLU) receptors can stimulate the production of NO in various cellular and subcellular locations in the retina (Blute et al., 2000), and nicotine can activate both the production of NO and cGMP in separate but overlapping populations of retinal neurons (Blute et al., 2003). Virtually all amacrine cells have either GABA or glycine (GLY; Marc et al., 1995; Kalloniatis et al., 1996), and neuronal nitric oxide synthase (nNOS) has been shown to colocalize with either GABA or GLY in amacrine cells (Haverkamp et al., 2000).

Our previous study suggested that GLY may participate in inhibitory pathways (Yu & Eldred, 2005) involving glycine receptor (GLYR), $GABA_A$, and $GABA_C$ receptors ($GABA_A$Rs and $GABA_C$Rs). Such inhibitory pathways and the reciprocal inhibitory relationship between GABA and GLY are well documented in the retina (Zhang et al., 1997; Dong & Werblin, 1998; Shen & Slaughter, 2001), but their contributions to the regulation of the NO/cGMP signaling pathway remains unclear. The experiments described in this report were designed to clarify the interactions between GLY and GABA in the modulation of the NO/cGMP signaling pathways.

In these experiments, we used glycinergic and GABAergic antagonists to selectively block the effects of inhibition through each pathway, and then observed changes in NO production and cGMP levels using a NO-imaging technique (Blute et al., 2000) and cGMP immunocytochemistry. Our results indicate that GABA and GLY interact to modulate the NO/cGMP signaling pathways in the retina.

Materials and methods

Reagents

All reagents were from Sigma-Aldrich Chemical Company(St. Louis, MO) with the following exceptions: citric acid and sodium citrate dihydrate (J.T. Baker Inc., Phillipsburg, NJ); (Z)-1-[2-(2-Aminoethyl)-N-(2-ammonioethyl)amino]diazen-1-ium-1,2-diolate (DETA, Alexis USA., San Diego, CA); hydroquinone (Eastman Kodak Co., Rochester, NY); silver nitrate (Fisher Scientific Co., Fair Lawn, NJ); 4 nm colloidal gold goat-anti-rabbit IgG (Jackson ImmunoResearch, West Grove, PA); Vector Elite™ avidin-biotin complex (ABC) reagents (Vector Laboratories, Inc., Burlingame, CA); and Immunopure™ metal-enhanced diaminobenzidine (DAB) substrate (Pierce Chemical Company, Rockford, IL). The NO-sensitive fluorescent dye 4,5-diaminofluorescein diacetate (DAF-2DA) was from Calbiochem (San Diego, CA). The rabbit polyclonal antisera against GABA and GLY were kind gifts from Dr. David V. Pow (Vision, Touch and Hearing Research Centre, Department of Physiology and Pharmacology, The University of Queensland, Brisbane, Queensland, Australia). The sheep and rabbit anti-cGMP antibodies were kind gifts from Dr. Jan de Vente (Department of Pharmacology, Faculty of Medicine, Free University, Amsterdam, Netherlands).

Tissue preparation and in vitro incubations

Adult turtles (*Pseudemys scripta elegans)* were maintained on a 12-h light/12-h dark cycle. A total of 18 animals were used for this study, and at least three animals were used for each of the pharmacological treatments. Near the middle of the light cycle, they were decapitated using a method approved by the Boston University Charles River Campus Institutional Animal Care and Use Committee. The enucleated eyes were hemisected along the vertical midline perpendicular to the visual streak. In the cGMP immunocytochemistry experiments and the double-labeling experiments with cGMP and either GABA or GLY antibodies, the eyecups were preincubated for 15 min in an aerated, balanced salt solution (BSS; 110 mM NaCl, 2.5 mM KCl, 3 mM $CaCl_2$,2mM $MgCl_2$, 10 mM glucose, and 5 mM HEPES, pH 7.4) at room temperature with 1 mM 3-isobutyl-1-methylxanthine (IBMX; a nonspecific phosphodiesterase inhibitor) prior to the pharmacological treatments. For NO-imaging experiments, the retinas were isolated from the eyecups, spread flat on a nitrocellulose filter, mounted on a glass slide, and then cut into 500-μm-thick slices before being loaded with the NO-sensitive fluorescent dye DAF-2DA.

Cyclic GMP immunocytochemistry

Following the preincubation in IBMX, the eyecups were transferred to fresh IBMX-BSS for 30 min with or without the following drugs: strychnine(STRY; 10-200 μM), bicuculline (BIC, 10-100 μM), (1,2,5,6-tetrahydropyridin-4-yl) methylphosphinic acid (TPMPA, 10-100 μM), (5R,10S)-(+)-5-methyl-10,11-dihydro-5H-dibenzo [a,d] cyclohepten-5,10-imine (MK801, a selective antagonist for NMDA receptors; 100 μM), 6-cyano-7-nitroquinoxaline-2,3-dione (CNQX, a selective antagonist for AMPA/KA receptors, 100 μM), or the NOS inhibitor S-methyl-L-thiocitrulline(SMTC, 100 μM). STRY is an antagonist for GLY receptors (White, 1985), BIC is an antagonist for $GABA_A$ receptors ($GABA_A$Rs; Shields et al., 2000), and TPMPA is a specific antagonist for $GABA_C$R (Ragozzino et al., 1996). The following combinations of treatments were also done for 30 min: 100 μM STRY with 100 μM TPMPA; 100 μM STRY with 100 μM BIC; 100 μM STRY with 100 μM SMTC; 100 μM STRY with 100 μM MK801; 100 μM STRY with 100 μM CNQX; or 100 μM STRY with both 100 μM MK801 and 100 μM CNQX. As control treatments, the effects of just IBMX-BSS and SMTC-BSS alone were also tested. All incubations were done in normal room light.

Following the pharmacological incubations, the eyecups were fixed with 4% paraformaldehyde in 0.1 M phosphate buffer, pH 7.4 (PB), for 120 min. After fixation, the eyecups were cryoprotected using a sucrose series, embedded and frozen in OCT (optimum cutting temperature) embedding compound, and cut using a cryostat into 14-μm-thick cross sections that were thaw-mounted onto slides subbed with chrome gelatin.

All antisera solutions were diluted in 0.1 M PB with 0.3% Triton X-100 at pH 7.4. To control for nonspecific labeling, sections were pretreated with 2% normal goat serum for 60 min at room temperature in a moist dark chamber. The sections were then incubated overnight in a 1:5000 dilution of rabbit antibody raised against cGMP. The production, characterization, and specificity of this antibody have been described previously (de Vente & Stein-busch, 1992). The sections were subsequently labeled using standard immunocytochemical techniques employing Vector Elite™ ABC reagents (diluted 1:1000) and Immunopure™ Metal Enhanced DAB substrate. Digital images were acquired using a CCD camera (Apogee Instruments Inc., Auburn, CA) and MaximDL™ software (Cyanogen Productions Inc., Ottawa, ON, Canada) at 400× magnification.

NO imaging and quantitative analysis

The retinal slices were loaded with 10 μM DAF-2DA in a dark chamber for 1 h. After a 1-h wash in aerated BSS in a dark chamber, the slices were subjected to one of the following

pharmacological treatments for 5 min (all drugs were used at 10- 100 μM): STRY alone; BIC alone; TPMPA alone; NMDA alone; MK801 alone; CNQX alone; STRY with BIC; STRY with TPMPA; STRY with MK801; STRY with CNQX; or BIC with TPMPA. The slices were then fixed in 4% paraformaldehyde in 0.1 M phosphate buffer (PB, pH 7.4) for 30 min immediately after the treatments, and they were then observed using a Fluoview™ 300 confocal microscope (Olympus Corporation, Melville, NY) to image the NO-induced fluorescence (NO-IF). Data images were acquired in 10 × 1 μm-step Z-stacks using the Fluoview™ software (Olympus Corporation, Melville, NY) to reduce the sampling variability associated with different focal planes that are frequently associated with single focal plane images. The Z-stack images were then collapsed to single frames using Image-Pro Plus™ software (Media Cybernetics Inc., Carlsbad, CA) to obtain the total labeling found in the Z-stack. Since the quantitative comparisons of the effects of different pharmacological treatments needed to be based on the levels of NO-IF produced in comparable retinal slices, it was essential to control the sample images such that the quantitative measurements were based on images of retinal samples with the same dimensions. All images were taken at the same magnification and any variables due to retinal thickness and length were minimized by careful choice of the specific retinal slices quantified such that each experimental or control retinal slice had comparable dimensions. To further minimize variables due to minor variations in the dimensions of the chosen retinal samples, such as curvature, a fixed-size rectangular selection tool was used in Adobe Photoshop™ software (Adobe Systems, Mountain View, CA) to obtain retinal images with precisely the same dimensions. The optical density sum (ODS) of the NO-IF in each retinal sample image was then measured using Image-Pro Plus™. The specific mathematical formulas used to compare the effects of different pharmacological treatments are described in the Results section. Statistical comparisons of the ODS values measured with the different treatments were analyzed using an ANOVA Dunnett's Test (XLStat Pro™ plug-in, Addinsoft, Brooklyn, NY, for Excel™, Microsoft, Redmond, WA). All quantified data are presented as means ± SEM. All significance claims are based on $P < 0.01$ unless noted otherwise. The images were then arranged and labeled using Corel Photo-Paint™ and Corel Draw™ software (Corel Corporation, Ottawa, ON, Canada).

Double labeling of cGMP with GABA or GLY

The eyecups were treated with the NO donor DETA (200 μM) for 60 min in the presence of 1 mM IBMX, before they were processed as described for the cGMP immunocytochemistry. The retinal sections on the slides were incubated in 2% normal goat serum and 2% normal donkey serum for 1h to eliminate nonspecific labeling prior to an overnight incubation with the combination of 1:5000 sheep anti-cGMP antibody with either 1:10,000 rabbit anti-GABA or 1:10,000 rabbit anti-GLY antibody. A mixture of Cy5-labeled goat-anti-rabbit secondary antibody (1:1000) and Alexa 488-labeled donkey-anti-sheep secondary antibody (1:1000) was applied to the slides for 1 h after thorough washes. The slides were then washed again before observation using confocal microscopy. Two individual lasers (648 nm and 488 nm) were used to excite the two distinct secondary antibodies so that the labeling of each antibody was captured in a separate channel. There was no staining seen when sections were incubated with either of the secondary antibodies alone or any cross-reactivity when the sections were incubated with both secondary antibodies and only one of the primary antibodies. Images were acquired and processed as described in the NO-imaging section, and the uniformity of the sample images were controlled as described previously. However, since these images were captured from 14-μm-thick cryostat sections, any differences in focal plane were not a significant variable, so Z-stacks were not used. The total ODS_{cGMP} was measured in the Alexa 488 channel (green), and the double-labeled ODS_{cGMP} was measured in images processed mathematically from both the Cy5 channel image and the Alexa 488 channel image to show the double labeled (overlapping) signals in both channels using the Adobe Photoshop™ Math

function. The percentage of double-labeled cGMP signal in the total cGMP signal in each dual channel image was then calculated.

Results

Our previous studies indicate that GABAergic inhibitory pathways regulate NO/cGMP signaling through a serial inhibitory circuit that involves both inter-amacrine inhibition through $GABA_AR$, and feedback inhibition to bipolar cell axon terminals through $GABA_CR$ (Yu & Eldred, 2005). These results led to the hypothesis that $GABA_CR$-mediated pathway may regulate the levels or temporal properties of inter-amacrine glycinergic inhibition onto NO-producing cells. To investigate the roles of glycinergic inhibition on the NO/cGMP signaling pathway, we have now selectively blocked GLYR and observed the effects on the production of NO and cGMP. Our previous study used cGMP-LI to gauge the effects of GABAergic inhibition on the NO/cGMP pathway, but it could not localize the sites of the inhibitory effects to specific aspects of the NO-cGMP signaling cascade. In the present study, we addressed this issue by using a combination of cGMP immunocytochemistry and NO-imaging techniques (Blute et al., 2000) to monitor the effects of blocking GLYR on cGMP production and to directly monitor the effects on NO production.

Cyclic GMP immunocytochemistry

Strychnine increased cGMP-LI in select cell types but showed regional differences—Like GABA, GLY is also a widely distributed inhibitory transmitter in the retina (Eldred & Cheung, 1989; Marc et al., 1995).To test our hypothesis that GLY also inhibits the NO/cGMP signaling pathways, we blocked the glycinergic inhibition using STRY. In sharp contrast to control retinas, which had virtually no detectable endogenous cGMP-LI (Fig. 1A), STRY (10-200 μM) dose dependently increased cGMP-LI in select cell types and their processes in the inner plexiform layer (IPL) (Figs. 1B-1H) with the most effective concentration being 100 μM. The stratification within the IPL of the retinal cross sections is described such that the border between the inner nuclear layer (INL) and the IPL is S0, the middle of the IPL is S50, and the border between the IPL and the ganglion cell layer (GCL) is S100.

All cell types with elevated cGMP-LI in response to STRY stimulation had monostratified arborizations in the IPL. All the known soluble guanylyl cyclase (sGC) cell types in turtle retina have been reported previously (Blute et al., 1998) and they were classified on the basis of the localization of their somata in the INL and their dendritic arborizations in the IPL. The following sGC containing amacrine cell types showed elevated cGMP-LI in response to STRY: sGC A1, sGC A2, sGC A3, sGC4, and sGC A11. However, the predominant cell type was sGC A2. Soluble GC A1 amacrine cells had pyriform-shaped somata in the second tier of the INL that extended a single primary dendritic process that arborized near S15-S30 of the IPL (Fig. 1B). Soluble GC A2 cells had large rounded somata that were found in the first tier of the INL adjacent to the IPL and gave rise to a single primary process that also arborized near S15-S30 of the IPL (Fig. 1C). Soluble GC A3 amacrine cells had small somata located in the first tier of the INL (Fig. 1D), and gave rise to a single primary process that branched in S50-S60 of the IPL. Only in the inferior retina (retina below the visual streak) could sporadic sGCA4 cell types be found. These cells were characterized by their displaced pyriform-shaped somata in the GCL (Fig. 1E). Very rarely, sGC A11 cells were seen in the superior retina above the visual streak, with flattened somata located in the first tier of the INL that gave rise to two primary processes that arborized in S20-S30 of the IPL (Fig. 1G). Occasionally, some bipolar cells resembling the sGC B1 and B2 types were seen, but mostly in the inferior retina (Figs. 1B & 1H).In sharp contrast to the effects of bicuculline (Yu & Eldred, 2005), with strychnine there were very few bipolar cells showing elevated cGMP-LI in the central retina.

Elevated cGMP-LI was also present in dendritic processes in the IPL, forming clearly labeled bands in both the ON or OFF strata of the IPL (Figs. 1B-1H; Ammermüller & Kolb, 1995). However, the banding patterns varied based on region. In the superior retina, cGMP-LI was seen in S15-S30 and S80 of the IPL (Figs. 1C & 1F). In the inferior retina, the bands were most visible in S15-S30 and S60 near the visual streak (Figs. 1D & 1E), but the band at S60 disappeared toward the ora serrata (Figs. 1B & 1H). In the central retina near the visual streak, there were few labeled somata and the bands were barely visible in S20 and S65 of the IPL (Fig. 1G).

NO production and GLU were both involved in STRY increased cGMP-LI—To test whether the STRY-stimulated increases in cGMP-LI involved NO production, we incubated retinas with STRY and the NOS inhibitor SMTC. SMTC completely eliminated the effects of STRY on cGMP-LI, and Fig. 2B shows no cGMP-LI anywhere in the retina in the presence of 100 μM SMTC. This shows that NO production was activated by STRY.

To test whether GLU had a role in the effects of STRY, we stimulated the retinas with STRY in the presence of selective antagonists for ionotropic GLURs. Coincubation with 100 μM CNQX completely blocked the effects of STRY on cGMP-LI (Fig. 2C), and 100 μM MK801 caused some reduction of the effects of STRY (Fig. 2D). Costimulation with all three drugs had the same effects as CNQX with STRY (Fig. 2E). All images presented were taken from mid-inferior retinas, between the visual streak and the inferior ora serrata. This suggests that glycinergic inhibition has a strong effect on NO/cGMP synaptic pathways involving AMPA/KA receptors.

GABAergic inhibitory pathways interact with glycinergic inhibition of cGMP-LI—To investigate the influence of GABAergic inhibition in the role of GLY, we combined STRY with antagonists for GABA receptors. Coincubation with 100 μM STRY and 100 μM of the $GABA_AR$ antagonist BIC dramatically increased cGMP-LI in the retina, giving a NO-donor-like response in that many amacrine and bipolar cell types showed elevated cGMP-LI and their dendritic processes were strongly labeled (Fig. 2F). However, coincubation with 100 μM of the $GABA_C$ receptor ($GABA_CR$) antagonist TPMPA dramatically decreased the STRY-stimulated increases in cGMP-LI in most cell types and dendritic processes in the IPL (Fig. 2G). Coincubation with all three drugs produced increases in cGMP-LI that resembled those seen with BIC alone (Yu & Eldred, 2003), although they were somewhat weaker (Fig. 2H). These experiments show that $GABA_AR$ mediates a stronger inhibition with a wider impact than does GLYR on cGMP production, and that TPMPA enhanced the reciprocal inhibition between GABAergic and glycinergic neurons. However, the question of where such serial inhibitory modulation occurs demanded more information about the role of NO production.

NO-imaging experiments

To compare the effects of the inhibitory pathways on NO production with the effects on cGMP-LI, we used a NO-specific fluorescent probe, DAF-2DA, to directly monitor the production of NO in response to the antagonists of GLYR and GABA receptors. The application of DAF-2DA to image NO in the retina has been described previously (Blute et al., 2000), and both NMDA and nicotine have been shown to stimulate strong NO production in select cellular and subcellular locations across the retina (Blute et al., 2000, 2003). To evaluate the efficacy of each treatment (E_X) for the stimulation of NO production, we used the effects of NMDA as a standard and defined the efficacy of NMDA (E_{NMDA}) as 100%: $E_{NMDA} = (ODS_{NMDA} = ODS_{Control}) \times 100\%/(ODS_{NMDA} = ODS_{Control}) = 100\%$ (Fig. 4). NMDA was chosen as a standard to allow comparison with our previous study examining the effects of bicuculline on cGMP in retina (Yu & Eldred, 2003). ODS_{NMDA} is the average optical density sum of the NO-IF from five retinal slices from the same animal stimulated using 100 μM NMDA, and

$ODS_{Control}$ is the average optical density sum of the NO-IF from five unstimulated retinal slices from the same animal. The final E_X values were means of results from three animals ($N = 3$), and all data are presented as means ± SEM. The efficacies of the other treatments (X) were defined as: $E_X = (ODS_X = ODS_{Control}) \times 100\%0 (ODS_{NMDA} = ODS_{Control})$.

To effectively compare the effects on cGMP production and NO production, we used the same dosages of drugs for both experiments. Since significant increases in NO-IF were observed within 2-3 min in NMDA-treated retinal slices (Blute et al., 2000), we did time-course experiments for all pharmacological treatments ranging from 1-15 min. Longer stimulations (>7 min) brought up the background significantly, while shorter stimulations (<2 min) did not show the full effects as different cells had different kinetics and their peaks of NO-IF occurred with different time courses. In the case of NMDA, it has been shown that the peaks of NO-IF in ganglion cells, amacrine cell somata, and synaptic boutons in the IPL were reached in 2-7 min (Blute et al., 2000). Therefore, we chose 5-min stimulations for all treatments to minimize differences due to different kinetics in various cell types and pharmacological treatments.

GLYR and GABAR antagonists had different effects on NO production—In unstimulated control retinal slices, there were only background levels of NO-IF ($E_{Control} = 0 \pm 24\%$; Figs. 3A & 4). NMDA (100 μM) stimulated strong increases in NO-IF ($E_{NMDA} = 100 \pm 18\%$; Figs. 3B & 4), in agreement with a previous study (Blute et al., 2000). STRY (100 μM), however, also stimulated strong NO production in numerous somata in the INL and GCL, as well as in synaptic boutons in the IPL ($E_{STRY} = 85 \pm 16\%$; Figs. 3C & 4). These somata were most likely to be amacrine cells with NO-IF and displaced amacrine cells. Small numbers of labeled bipolar and ganglion cells were also seen. BIC (100 μM) also stimulated significant NO production in comparison to the control retinas, however, the levels of NO production and the numbers of activated cells were roughly half of what STRY stimulated at the same dose ($E_{BIC} = 43 \pm 11\%$; Figs. 3D & 4). TPMPA (100 μM) did not stimulate any significant increases in NO-IF ($E_{TPMPA} = 10 \pm 9\%$; Figs. 3E & 4), which is in agreement with its weak effects on cGMP-LI (Yu & Eldred, 2003). The combination of STRY and BIC (both 100 μM) stimulated relatively high levels of NO-IF ($E_{STRY+BIC} = 112 \pm 12\%$; Figs. 3F & 4). In sharp contrast to the effects on cGMP-LI, coincubation with STRY and TPMPA (both 100 μM) did not decrease the levels of NO-IF in comparison to STRY alone ($E_{STRY+TPMPA} = 92 \pm 19\%$; Figs. 3G & 4). The combination of BIC and TPMPA (both 100 μM) did not significantly differ from the effects of BIC alone ($E_{BIC+TPMPA} = 38 \pm 15\%$; Figs. 3H & 4), although there were fewer labeled somata in the GCL with BIC and TPMPA .

These findings suggest that GLY and GABA may control separate populations of nNOS-containing cells, with GLY playing a more prominent role in inhibiting NO production. The differences between the effects on cGMP-LI and NO-IF indicate a differential modulation of the NO production and cGMP production by GLY and GABA (Table 1).

Specific GLURs were involved in the effects of STRY—To investigate the involvement of GLU in the effects of STRY, we coincubated the retinal slices with the selective GLUR antagonists CNQX and MK801. Neither CNQX nor MK801 alone (100 μM each) increased the NO-IF significantly ($E_{CNQX} = 11 \pm 5\%$, $E_{MK-801} = 13 \pm 7\%$; Figs. 3I, 3J, & 4). The addition of 100 μM CNQX, however, significantly reduced the effects of STRY ($E_{STRY+CNQX} = 15 \pm 10\%$; Figs. 3K & 4), while 100 μM MK801 did not ($E_{STRY+MK-801} = 105 \pm 7\%$; Figs. 3L & 4).

Colocalization of cGMP with GABA or GLY

Our results indicate that GABA and GLY had different effects on cGMP-LI. Furthermore, STRY stimulated strong NO production but had weaker effects on cGMP-LI, while BIC

produced the opposite results. Based on the reciprocal inhibitory relationship between GABA and glycine, sGC colocalized with GABA is likely to be under glycinergic inhibition, and sGC colocalized with GLY is likely to be under GABAergic inhibition. Given that GABA and GLY cells can inhibit each other and all amacrine cells express either GABA or GLY, these results may be due to the difference in the distribution of sGC in amacrine cells containing GABA versus GLY. Since synapses formed by dendritic processes in the IPL are the primary sites of cell-to-cell communication, not the somata, the fact that numerous synaptic boutons showed increased cGMP-LI in response to NO stimulation suggests that the GLYR- or GABAR-mediated inhibition may modulate the production of cGMP at the synaptic level. Therefore, we did not just count the double-labeled cell somata to compare the colocalization of cGMP-LI with GLY or GABA, but instead measured the colocalization throughout all layers of the retina, which would include all synaptic boutons.

Fig. 5A shows the immunofluorescent labeling of GABA-LI, cGMP-LI, and their colocalization, while Fig. 5B shows the immunofluorescent labeling of GLY-LI, cGMP-LI, and their colocalization. To quantitatively compare the percentage of the double-labeled cGMP-LI to the total cGMP-LI, the ODS of each image of retinal regions with comparable dimensions was measured (see Materials and methods). The data comparisons were based on the same total ODS_{cGMP} level for each experiment and the antibody dilutions for GABA and GLY were the same. An average of ten samples each for three animals confirmed that 76±5% of the NO donor-stimulated increase in cGMP-LI colocalized with GLY, whereas only 13±2% colocalized with GABA.

Discussion

Modulation of NO/cGMP production by synaptic inhibition

In this study, we show that selectively blocking glycinergic inhibition using STRY caused moderate increases in cGMP-LI, in sharp contrast to the larger increases seen with BIC (Yu & Eldred, 2005; Table 1). The effects of STRY and BIC on NO-IF were largely opposite of their effects on cGMP production, in that quantitative analysis indicated that STRY stimulated roughly twice as much NO-IF as BIC did in the same time frame. Two factors may be the most important for causing such disparities. One factor being the extent of the colocalization of GABA or GLY with either NOS or sGC. The second factor being the distances between the sites of NO production in NOS-positive synaptic boutons and the sites of cGMP production in sGC-positive synaptic boutons.

Extent of localization of NOS or sGC in GABA or GLY cells—The synaptic localization of NOS determines which type of inhibitory inputs may control the production of NO. GABAergic and glycinergic amacrine cells can inhibit each other (Zhang et al., 1997; Dong & Werblin, 1998; Shen & Slaughter, 2001), and all amacrine cells contain either GABA or GLY (Marc et al., 1995; Kalloniatis et al., 1996). On the basis of these reciprocal interactions, blocking $GABA_AR$ with BIC should activate NO production in glycinergic nNOS cells, and blocking GLYR with STRY should activate increases in NO-IF in GABAergic nNOS cells. A previous study reported that nearly equal numbers of GABAergic and glycinergic amacrine cell somata contained NOS (Haverkamp et al., 2000). However, the difference between the effects of BIC and STRY on NO production suggests that there is a difference in the number of synaptic boutons that express both NOS and GABA or GLY.

Although both GABAergic and glycinergic amacrine cells can have large or small dendritic arborizations, glycinergic amacrine cells have primarily small field arborizations in cat (Pourcho & Goebel, 1985) and human retina (Crooks & Kolb, 1992). In salamander retina, however, glycinergic amacrine cells have primarily large dendritic fields (Yang et al., 1991). Therefore, there may be large differences between GABAergic and glycinergic neurons in the

number of synaptic boutons that express NOS, due to the differences in the average size of their dendritic arborizations. Although it is unclear whether the glycinergic amacrine cells in the turtle retina are primarily large field cells or small field cells, the stronger NO production in response to STRY clearly suggests that there are more NOS-positive synaptic boutons receiving glycinergic inhibition than the ones receiving GABAergic inhibition.

Localization of NOS versus sGC—On the basis of the NO-imaging studies done in the past (Blute et al., 2000) and the present study, we can clearly see that NO does not diffuse very far from its sites of production. In fact, most synaptic boutons that showed high levels of NO-IF in the IPL demonstrated very limited spread of the NO-IF even over long time periods (Blute et al., 2000). Therefore, the resulting increases in cGMP production in boutons must be within the diffusion range of the NO producing synapses. The different effects of STRY and BIC on cGMP production may reflect the differences in distance between synaptic boutons expressing sGC and the sites of NO production in response to BIC or STRY. If the glycinergic NOS positive synaptic boutons are closer to synaptic boutons that express sGC, then blocking GABAergic inhibition of the glycinergic NOS-positive synaptic boutons with BIC may produce less NO but activate stronger cGMP production. In contrast, if the GABAergic NOS-positive synaptic boutons are further from synaptic boutons that express sGC, then blocking glycinergic inhibition of GABAergic NOS-positive synaptic boutons with STRY may release more NO but activate less cGMP production.

Our double-labeling results show that sGC primarily colocalizes with GLY, and we show that NO can stimulate cGMP production in glycinergic cells. These results suggest that NO may influence glycinergic neurotransmission primarily through cGMP-dependent mechanisms, although it may also have affects on neurotransmission other than cGMP-dependent effects. This is supported by our previous study on the effects of NO and cGMP on GABA and GLY release and uptake in turtle retina (Yu & Eldred, 2005). We found that NO donor or cGMP both decreased release of glycine in the IPL, while in contrast we found that both NO donor, and to a lesser extent cGMP, increased GABA release in the IPL. Finally, the differences we see in cGMP-LI in response to stimulation with STRY or BIC suggest that NO modulates signal transduction in precise synaptic pathways, as opposed to the more commonly accepted idea that it is freely diffusible. If NO was freely diffusible, there would be little difference in the postsynaptic production of cGMP in response to NO from different synaptic sources.

It also remains a possibility that there could be GABAergic or glycinergic inhibition of cGMP production in sGC-containing cells. Even though NO does not apparently diffuse over long distances, it is very likely it can diffuse from its cellular sources to activate sGC in synaptic boutons that are within the NO diffusion range from its source. Zabel et al. (2002) show that Ca^{2+}-dependent translocation to the cell membrane sensitizes sGC for activation by NO. Activation of the GLYR and $GABA_AR$ may inhibit depolarization-induced Ca^{2+} influx, therefore reducing the likelihood of sGC translocation to the membrane and reducing the activation of sGC in response to NO.

Regional differences in the NO/cGMP signaling pathways

Previous studies have shown distinct regional differences in the NO/cGMP pathways in retina. For instance there were clear regional differences in the cells with NMDA-stimulated increases in cGMP-LI in terms of the labeled cell types and their intensity of cGMP-LI (Blute et al., 1999). Below the visual streak, the overall intensity of cGMP-LI in the IPL increased toward the inferior ora serrata and there were robustly labeled displaced bipolar cells, most likely sGC B2 bipolar cells. However, above the visual streak, there were few bipolar cell somas with increased cGMP-LI in NMDA-stimulated retinas. Amacrine cell types sGC A3 and sGC A11 were also most frequently observed in the inferior retina.

Although there are several possibilities for these regional differences, there have been no reported regional differences in the following: specific GABA receptor subtypes (frog and turtle, Vitanova et al., 2001; salamander, Yang et al., 1992; rat, Greferath et al., 1993, Enz et al., 1996),NOS (Blute et al., 1997),sGC (Blute et al., 1998), or NMDA and AMPA/KA receptor subtypes (Grünert et al., 2002). Blute et al. (1998) also examined the effects of the nonspecific phosphodiesterase inhibitor IBMX and found no obvious regional effects. The present study does show regional effects of stimulation with STRY in that there were more sGCA4 cells and B1 and B2 bipolar cells below the visual streak. These results suggest that glycinergic inhibitory synaptic mechanisms may be responsible for at least some regional differences in the NO/cGMP signaling pathways in retina.

Integration of the glycinergic and GABAergic inhibitory pathways

Our previous study (Yu & Eldred, 2003) examined the effects of $GABA_AR$ and $GABA_CR$ antagonists on levels of cGMP-LI in turtle retina. The results of this study indicated that the $GABA_AR$ antagonist BIC caused strong increases in cGMP-LI. The $GABA_AR0$ $GABA_CR$ antagonist picrotoxin caused less of an increase in cGMP-LI and the $GABA_CR$ antagonist TPMPA had relatively little effect on cGMP-LI. These BIC-stimulated increases in cGMP-LI were reduced by MK801, largely blocked by CNQX, and effectively eliminated by the combination of MK801 and CNQX (Yu & Eldred, 2003). $GABA_CRs$ have been localized primarily on bipolar cell axon terminals (Lukasiewicz et al., 1994; Lukasiewicz, 1996; Koulen et al., 1997; Qian & Ripps, 2001). Based on the serial inhibition pathway described in the report by Zhang et al. (1997), enhancing $GABA_C$ feedback inhibition on bipolar axon terminals reduces their glutamate release. It naturally follows that eliminating the $GABA_C$ feedback inhibition on bipolar axon terminals would enhance the release of glutamate. Therefore, we speculated that the net effect of combining $GABA_CR$ antagonist TPMPA with bicuculline was to enhance the glutamate stimulated glycinergic inhibition of NO production (Yu & Eldred, 2003).

Although the production of cGMP often closely reflects the production of NO, it is also useful to focus directly on NO production (Fig. 3). The combination of STRY and MK801 (Fig. 3L) produced strong NO-IF, while CNQX almost completely eliminated STRY induced NO-IF (Fig. 3K). These experiments were in agreement with the cGMP immunocytochemistry, in that CNQX blocked the majority of the effects of STRY on cGMP production. These results suggest that AMPA/KA receptors are most responsible for the effects of STRY on NO production. Thus the effects of STRY could be due STRY blocking the GLY inhibition onto bipolar cells which increases their GLU release onto NOS-containing cells. This idea is supported by the fact that presumptive NOS amacrine cells have been shown to have either NMDA or kainate receptors(Sagar, 1990). Since the activation of AMPA/KA receptors is not voltage-dependent like NMDA receptors, these observations suggest that tonal modulation of presynaptic release underlies the glycinergic inhibition on nNOS activity.

In terms of the involvement of $GABA_AR$, $GABA_CR$, and GLYR in the modulation of the NO/cGMP signaling pathways there is consistency between the cGMP-LI and the NO-IF results. The combination of STRY and BIC increased the levels of both cGMP-LI and NO-IF in comparison to STRY alone. In contrast, the combination of STRY and TPMPA decreased NO-IF and almost completely eliminated cGMP-LI in comparison to STRY alone. These results would be consistent with BIC-sensitive $GABA_AR$ being on the NOS amacrine cells, and with GLYR- and TPMPA-sensitive $GABA_CR$ being on glutamatergic bipolar cell terminals that can also activate GABAergic amacrine cells. Therefore, STRY could increase glutamatergic activation of NO/cGMP production (Figs. 2A & 3C) and it could indirectly stimulate GABA release to inhibit NO production through $GABA_AR$ (Fig. 2F). This inhibition of STRY stimulated cGMP-LI through $GABA_ARis$ consistent with both the low levels of cGMP-LI in

the presence of STRY and TPMPA (Fig. 2G) and the increased levels of cGMP-LI in the presence of STRY, BIC, and TPMPA (Fig. 2H). The low levels of cGMP-LI (Yu & Eldred, 2003) and NO-IF (Fig. 3E) in response to TPMPA in comparison to BIC alone (Fig. 3D) would suggest strong basal levels of $GABA_AR$ inhibition, in addition to GLY inhibition of the NO/cGMP signaling pathway. Diagrammatic models of these pathways are presented in Fig. 6.

Conclusions

Our studies present inhibitory models (Fig. 6) that potentially integrate GABAergic and glycinergic inhibition at two levels along the NO/cGMP signaling pathway. At the level of NO production, GABA and GLY each inhibit a distinct group of nNOS-containing cells that also express either GLY or GABA. Blocking $GABA_AR$ or GLYR selectively activates cells with distinct GLUR distribution patterns with GLYR playing a dominant role in the inhibition of NO production. At the level of cGMP production, GABA plays a more dominant role in regulating the sensitivity of sGC-containing cells toward NO stimulation. The feedback inhibition onto bipolar cell axon terminals through $GABA_CR$ and GLYR and the reciprocal inhibition between GABA and GLY contribute to temporal and spatial diversity in regulation of the NO/cGMP signaling pathways. Our results establish anatomical and pharmacological models to be tested in future studies of the regulation of NO/cGMP in retinal physiology.

Acknowledgments

We wish to thank Dr. Todd A. Blute for his critical readings of the manuscript and many valuable discussions. We also want to thank Felicitas B. Eldred for her excellent technical assistance. This research was funded by the National Eye Institute, EY04785 (W.D.E.).

References

Ammermüller J, Kolb H. The organization of the turtle inner retina. i. on- and OFF-center pathways. Journal of Comparative Neurology 1995;358:1–34. [PubMed: 7560272]

Blute TA, Mayer B, Eldred WD. Immunocytochemical and histochemical localization of nitric oxide synthase in the turtle retina. Visual Neuroscience 1997;14:717–729. [PubMed: 9279000]

Blute TA, Velasco P, Eldred WD. Functional localization of soluble guanylate cyclase in turtle retina: Modulation of cGMP by nitric oxide donors. Visual Neuroscience 1998;15:485–498. [PubMed: 9685201]

Blute TA, De GRENIER J, Eldred WD. Stimulation with N-methyl-D-aspartate or kainic acid increases cyclic guanosine monophosphate-like immunoreactivity in turtle retina: Involvement of nitric oxide synthase. Journal of Comparative Neurology 1999;404:75–85. [PubMed: 9886026]

Blute TA, Lee MR, Eldred WD. Direct imaging of NMDA-stimulated nitric oxide production in the retina. Visual Neuroscience 2000;17:557–566. [PubMed: 11016575]

Blute TA, Strang C, Keyser KT, Eldred WD. Activation of the cGMP0nitric oxide signal transduction system by nicotine in the retina. Visual Neuroscience 2003;20:165–176. [PubMed: 12916738]

Crooks J, Kolb H. Localization of GABA, glycine, glutamate and tyrosine hydroxylase in the human retina. Journal of Comparative Neurology 1992;15:287–302. [PubMed: 1346792]

De VENTE J, Steinbusch HWM. On the stimulation of soluble and particulate guanylate cyclase in the rat brain and the involvement of nitric oxide as studied by cGMP immunocytochemistry. Acta Histochemica 1992;92:13–38. [PubMed: 1349785]

Devries SH, Schwartz EA. Modulation of an electrical synapse between solitary pairs of catfish horizontal cells by dopamine and second messengers. Journal of Physiology 1989;414:351–375. [PubMed: 2558170]

Dong CJ, Werblin FS. Temporal contrast enhancement via $GABA_C$ feedback at bipolar terminals in the tiger salamander retina. Journal of Neurophysiology 1998;79:2171–2180. [PubMed: 9535976]

Eldred, WD. Nitric oxide in the retina. Functional neuroanatomy of the nitric oxide system. In: Steinbusch, HWM.; De Vente, J.; Vincent, SR., editors. Handbook of Chemical Neuroanatomy. 17. Elsevier; New York: 2000. p. 111-145.

Eldred WD, Cheung K. Immunocytochemical localization of glycine in the retina of the turtle (Pseudemys scripta). Visual Neuroscience 1989;2:331–338. [PubMed: 2487656]

Enz R, Brandstatter JH, WÄssle H, Bormann J. Immunocytochemical localization of the GABAc receptor rho subunits in the mammalian retina. Journal of Neuroscience 1996;16:4479–4490. [PubMed: 8699258]

Greferath U, Muller F, WÄssle H, Shivers B, Seeburg P. Localization of GABAA receptors in the rat retina. Visual Neuroscience 1993;10:551–561. [PubMed: 8388246]

Grünert U, Haverkamp S, Fletcher EL, WÄssle H. Synaptic distribution of ionotropic glutamate receptors in the inner plexiform layer of the primate retina. Jouirnal of Comparative Neurology 2002;447:138–151.

Haverkamp S, Kolb H, Cuenca N. Morphological And Neurochemical Diversity Of Neuronal Nitric Oxide Synthase-Positive Amacrine Cells In The Turtle Retina. Cell and Tissue Research 2000;302:11–19. [PubMed: 11079711]

Ientile R, Pedale S, Picciurro V, Macaione V, Fabiano C, Macaione S. Nitric oxide mediates NMDA-evoked [^{3}H] GABA release from chick retina cells. FEBS Letters 1997;417:345–348. [PubMed: 9409748]

Kalloniatis M, Marc RE, Murry RF. Amino acid signatures in the primate retina. Journal of Neuroscience 1996;16:6807–6829. [PubMed: 8824321]

Koulen P, BrandstÄtter JH, Kroger S, Enz R, Bormann J, WÄssle H. Immunocytochemical localization of the GABA (C) receptor rho subunits in the cat, goldfish, and chicken retina. Journal of Comparative Neurology 1997;380:520–532. [PubMed: 9087530]

Kurenni DE, Thurlow GA, Turner RW, Moroz LL, Sharkey KA, Barnes S. Nitric oxide synthase in tiger salamander retina. Journal of Comparative Neurology 1995;361:525–536. [PubMed: 8550897]

Lukasiewicz PD. $GABA_C$ receptors in the vertebrate retina. Molecular Neurobiology 1996;12:181–194. [PubMed: 8884747]

Lukasiewicz PD, Maple BR, Werblin FS. A novel GABA receptor on bipolar cell terminals in the tiger salamander retina. Journal of Neuroscience 1994;14:1202–1212. [PubMed: 8120620]

Marc RE, Murry RF, Basinger SF. Pattern recognition of amino acid signatures in retinal neurons. Journal of Neuroscience 1995;15:5106–5129. [PubMed: 7623139]

Mills SL, Massey SC. Differential properties of two gap junctional pathways made by AII amacrine cells. Nature 1995;377:676–677. [PubMed: 7477255]

Miyachi E, Murakami MM, Nakaki T. Arginine blocks gap junctions between retinal horizontal cells. NeuroReport 1990;1:107–110. [PubMed: 2129864]

Ohkuma S, Katsura M, Chen DZ, Narihara H, Kuriyama K. Nitric oxide-evoked [^{3}H] gamma-aminobutyric acid release is mediated by two distinct release mechanisms. Brain Research Molecular Brain Research 1996a;36:137–144. [PubMed: 9011749]

Ohkuma S, Katsura M, Guo JL, Narihara H, Hasegawa T, Kuriyama K. Role of peroxynitrite in [^{3}H] gamma-aminobutyric acid release evoked by nitric oxide and its mechanism. European Journal of Pharmacology 1996b;301:179–188. [PubMed: 8773462]

Pourcho RG, Goebel DJ. A combined Golgi and autoradiographic study of (3H)glycine-accumulating amacrine cells in the cat retina. Journal of Comparative Neurology 1985;233:473–480. [PubMed: 2984258]

Prast H, Philippu A. Nitric oxide as modulator of neuronal function. Progress in Neurobiology 2001;64:51–68. [PubMed: 11250062]

Qian H, Ripps H. The $GABA_C$ receptors of retinal neurons. Progress in Brain Research 2001;131:295–308. [PubMed: 11420949]

Ragozzino D, Woodward RM, Murata Y, Eusebi F, Overman LE, Miledi R. Design and in vitro pharmacology of a selective gamma-aminobutyric acid C receptor antagonist. Molecular Pharmacology 1996;50:1024–1030. [PubMed: 8863850]

Sagar S. NADPH-diaphorase reactive neurons of the rabbit retina: Differential sensitivity to excitotoxins and unusual morphologic features. Journal of Comparative Neurology 1990;300:309–319. [PubMed: 2148324]

Savchenko A, Barnes S, Kramer RH. Cyclic-nucleotide-gated channels mediate synaptic feedback by nitric oxide. Nature 1997;390:694–698. [PubMed: 9414163]

Shen W, Slaughter MM. Multireceptor GABAergic regulation of synaptic communication in amphibian retina. Journal of Physiology 2001;530:55–67. [PubMed: 11136858]

Shields CR, Tran MN, Wong ROL, Lukasiewicz PD. Distinct ionotropic GABA receptors mediate presynaptic and postsynaptic inhibition in retinal bipolar cells. Journal of Neuroscience 2000;20:2673–2682. [PubMed: 10729348]

Shiells R, Falk G. Retinal on-bipolar cells contain a nitric oxide-sensitive guanylate cyclase. NeuroReport 1992;3:845–848. [PubMed: 1358250]

Vitanova L, Kupenova P, Haverkamp S, Popova E, Mitova L, WÄssle H. Immunocytochemical and electrophysiological characterization of GABA receptors in the frog and turtle retina. Vision Research 2001;41:691–704. [PubMed: 11248259]

White WF. The glycine receptor in the mutant mouse spastic (spa): Strychnine binding characteristics and pharmacology. Brain Research 1985;329:1–6. [PubMed: 2983837]

Yang CY, Lin ZS, Yazulla S. Localization of GABAA receptor subtypes in the tiger salamander retina. Visual Neuroscience 1992;8:57–64. [PubMed: 1310871]

Yang CY, Lukasiewicz P, Maguire G, Werblin FS, Yazulla S. Amacrine cells in the tiger salamander retina: Morphology, physiology, and neurotransmitter identification. Journal of Comparative Neurology 1991;312:19–32. [PubMed: 1683878]

Yu D, Eldred WD. $GABA_A$ and $GABA_C$ receptor antagonists increase retinal cyclic GMP levels through nitric oxide synthase. Visual Neuroscience 2003;20:627–638. [PubMed: 15088716]

Yu D, Eldred WD. Nitric oxide stimulates GABA release and inhibits glycine release in retina. Journal of Comparative Neurology 2005;483:278–291. [PubMed: 15682393]

Zabel U, Kleinschnitz C, Oh P, Nedvetsky P, Smolenski A, Muller H, Kronich P, Kugler P, Walter U, Schnitzer JE, Schmidt HH. Calcium-dependent membrane association sensitizes soluble guanylyl cyclase to nitric oxide. Nature Cell Biology 2002;4:307–311.

Zhang J, Jung CS, Slaughter MM. Serial inhibitory synapses in retina. Visual Neuroscience 1997;14:553–563. [PubMed: 9194322]

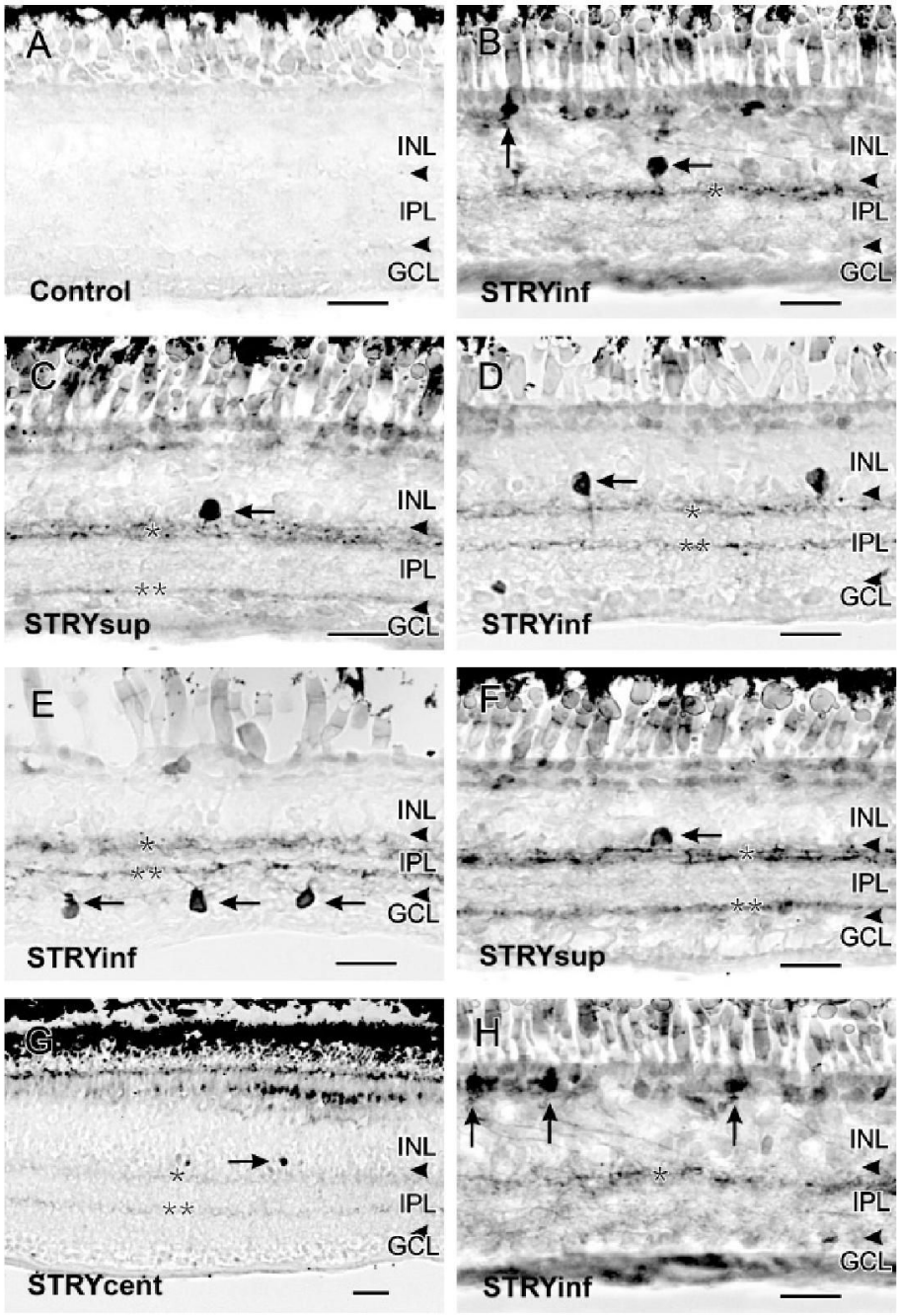

Fig. 1.

A: Control retinas had no cGMP-LI. B: In the inferior retina below the visual streak **(STRYinf)**, 100 μM strychnine increased cGMP-LI in sGC A1 amacrine cells (horizontal arrow) and sGC B2 bipolar cells (vertical arrow). A single band of cGMP-LI was present in S20 of the IPL (single asterisk) in the inferior retina close to the *ora serrata*. C: In the superior retina above the visual streak **(STRYsup)**,100 μM strychnine increased cGMP-LI in sGC A2 amacrine cells (horizontal arrow). Two labeled bands were present at S15-30 and S80 of the IPL (single and double asterisks). D: Labeled sGC A3 amacrine cells were seen in the inferior retina close to the visual streak (horizontal arrow). Two bands at S20 and S60 of the IPL were also visible (single and double asterisks). E: Labeled sGC 4 cells were seen in the GCL of the

inferior retina (horizontal arrows). F: Labeled A sGC A11 cells were seen in the superior retina (horizontal arrow). G: In the central retina**(STRYcent**), 100 μM strychnine stimulated increases in cGMP-LI in two faint bands at S20 and S65 of the IPL. Some GC A1-like amacrine cell somata were also seen (horizontal arrow). H: More bipolar cells with strong cGMP-LI were seen in the inferior retina (vertical arrows). Scale bars = 25 μm.

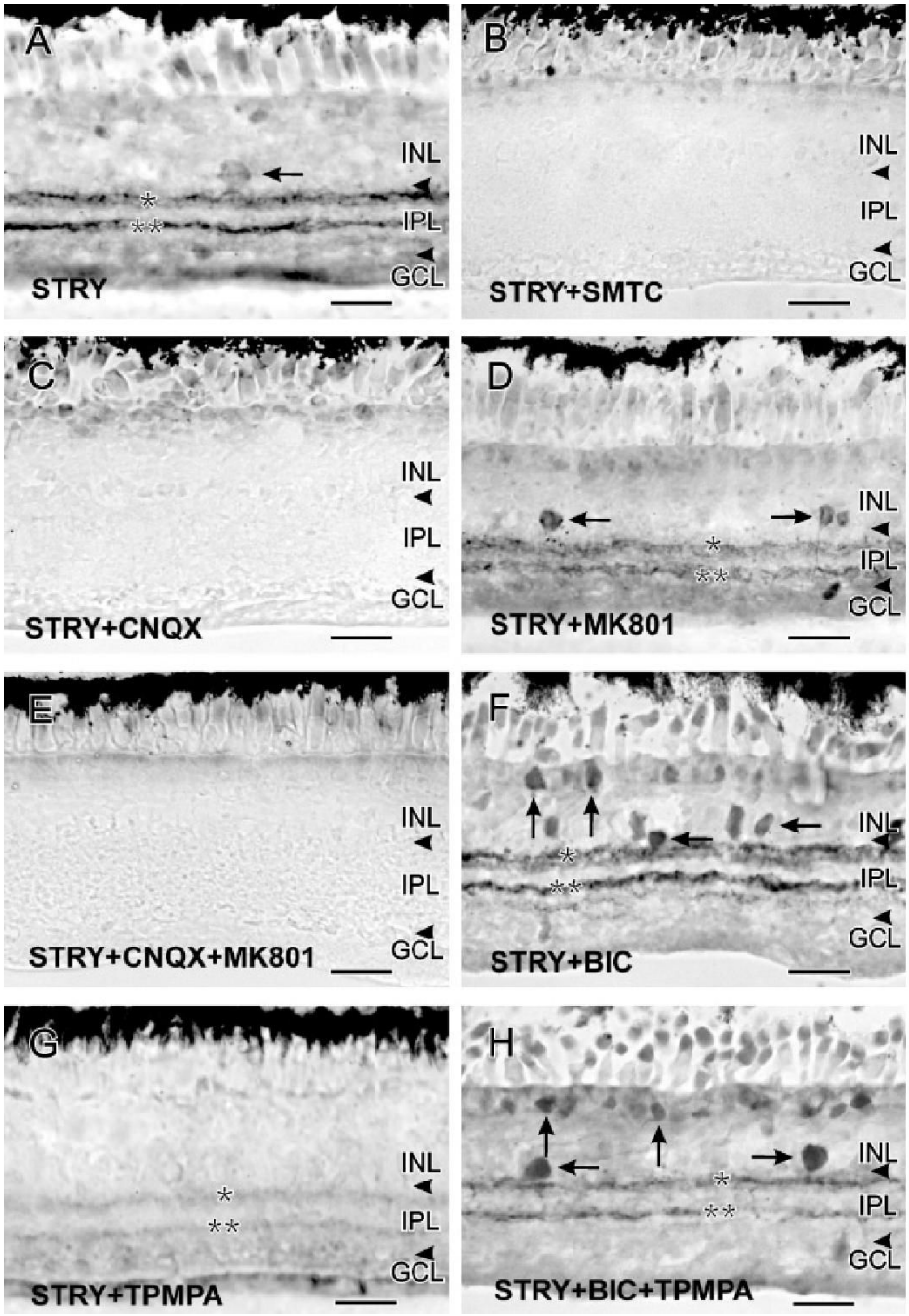

Fig. 2.

All images in this plate were captured from below the visual streak. A: 100 μM strychnine stimulated faint increases in cGMP-LI in sGC A2 amacrine cells (horizontal arrow) and in bands at S20 and S60 of the IPL. B: The NOS inhibitor SMTC blocked all STRY-stimulated increases in cGMP-LI. C: CNQX (100 μM) also blocked all the STRY-stimulated increases in cGMP-LI. D: MK801 (100 μM) did not block the effects of STRY on cGMP-LI, and there were still bands of cGMP-LI at S20 and S60 of the IPL (single and double asterisks) and in some labeled amacrine cells (horizontal arrows). E: The combination of STRY, CNQX, and MK801 mimicked STRY with CNQX. F: The combination of STRY and BIC (100 μM each) stimulated strong increases in cGMP-LI in bipolar cells (vertical arrows), amacrine cells

(horizontal arrows), and in S20 and S60 of the IPL (single and double asterisks). G: TPMPA (100 μM) reduced the effects of STRY, producing only very weakly labeled bands at S20 and S60 (single and double asterisks). H: The combination of STRY, BIC, and TPMPA resembled the combination of STRY and BIC, stimulating increases of cGMP-LI in bipolar (vertical arrows), amacrine cells (horizontal arrows), and in S20 and S60 of the IPL (single and double asterisks). Scale bars = 25 μm.

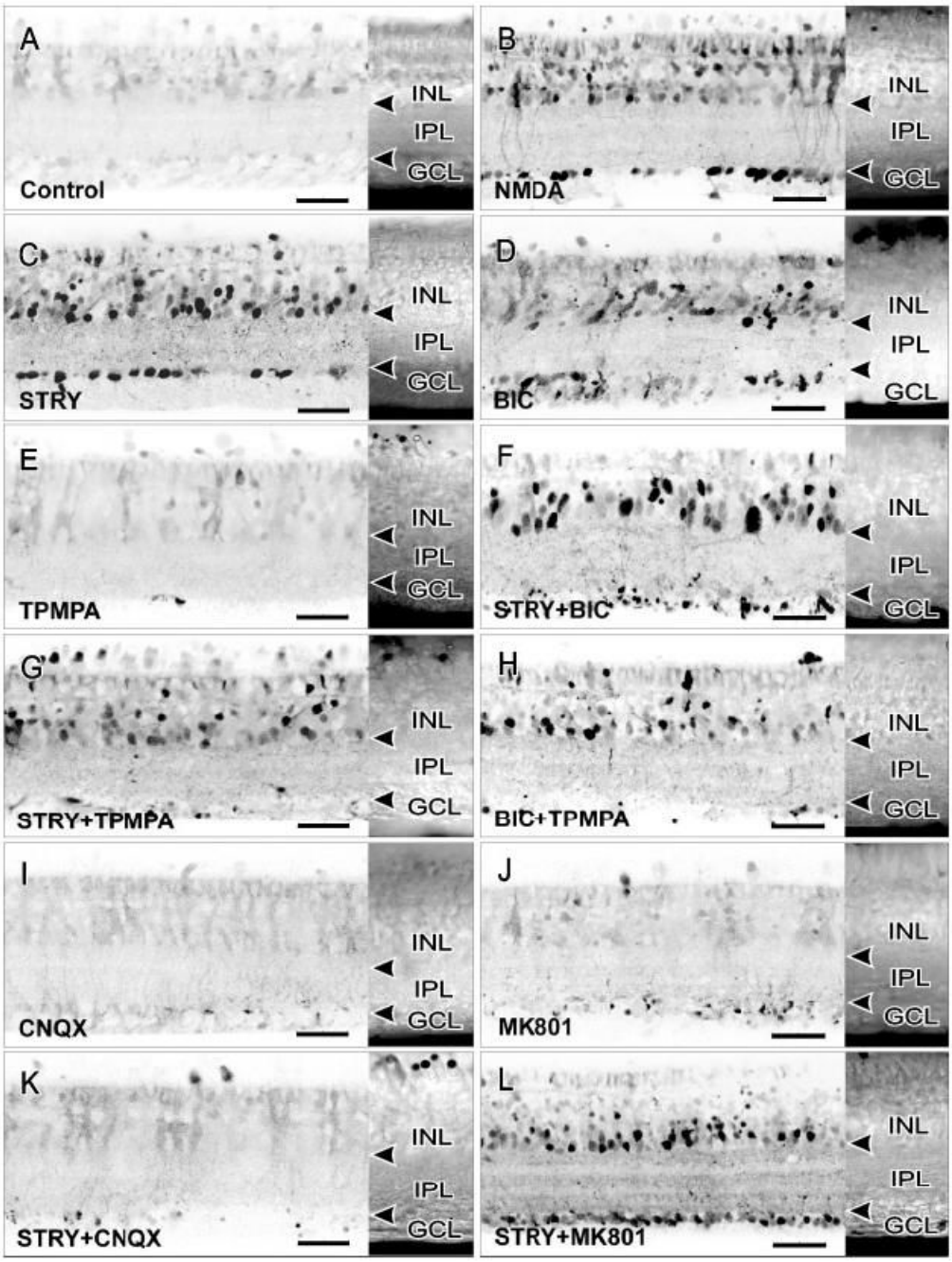

Fig. 3.

All drugs were used at 100 μM. A Nomarski image of each retinal slice is attached to the right of each contrast inverted image of NO-IF to show the layers of retinal neurons. Arrowheads indicate the borders of the IPL. A: Control retinas showed little endogenous NO production. B: NMDA stimulated strong increases in NO-IF in numerous somata in the ONL, INL, and GCL. Many synaptic boutons in the IPL (small dots in IPL) also showed strong increases in NO-IF. C: Stimulation with STRY resembled the effects of NMDA. D: BIC also stimulated an increase in NO-IF, although in fewer somata and synaptic boutons than did STRY. E: TPMPA alone had no obvious effect. F: The combination of STRY and BIC stimulated strong increases in NO-IF, similar to STRY alone or NMDA. G: TPMPA did not dramatically change

STRY-stimulated increases in NO-IF, although there were fewer labeled somata in the GCL. H: TPMPA also did not influence the effects of BIC except in the GCL. I: CNQX alone had no effect on NO-IF. J: MK-801 alone did not stimulate significant NO-IF increases. K: CNQX largely blocked the STRY-stimulated increases in NO-IF. L: MK801 had no obvious effects on STRY stimulated increases in NO-IF, with strong NO-IF in many somata and in the synaptic boutons in the IPL.

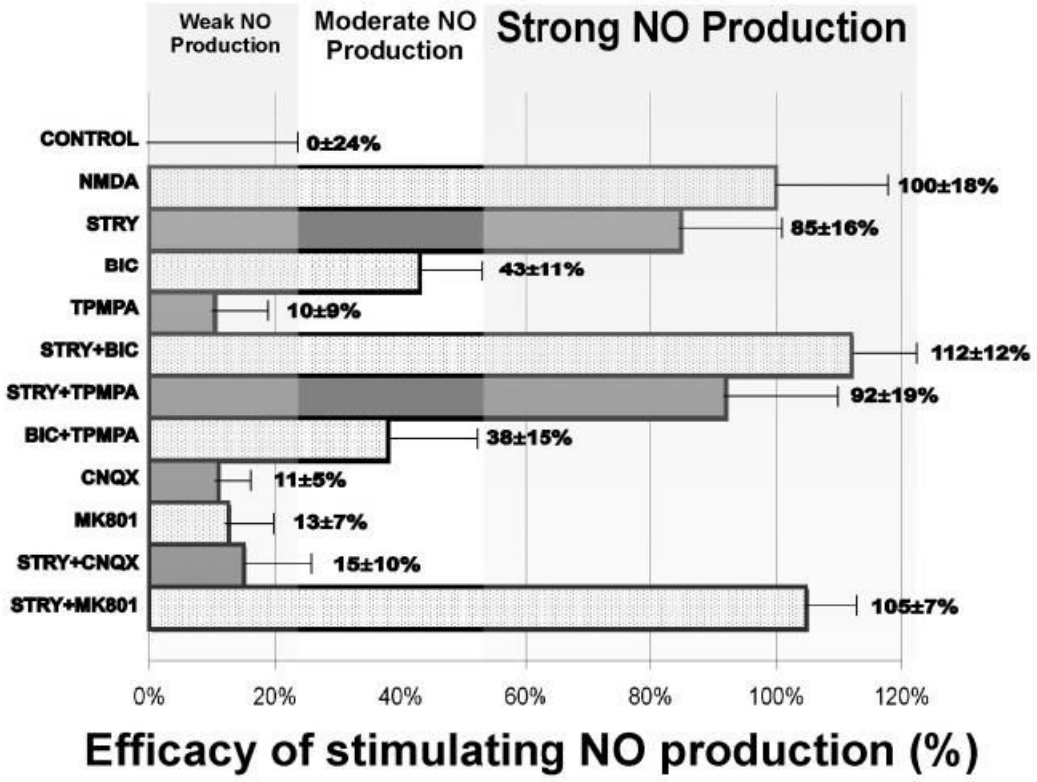

Fig. 4.

In comparison with the effects of NMDA in stimulating increases in NO-IF, which was taken to be 100%, the efficacy of each treatment in stimulating increases in NO-IF is shown in this figure. Each bar represents an average of 15 retinal slices from three different animals. The treatments were qualitatively grouped into three significantly different zones: weak NO production, moderate NO production, and strong NO production.

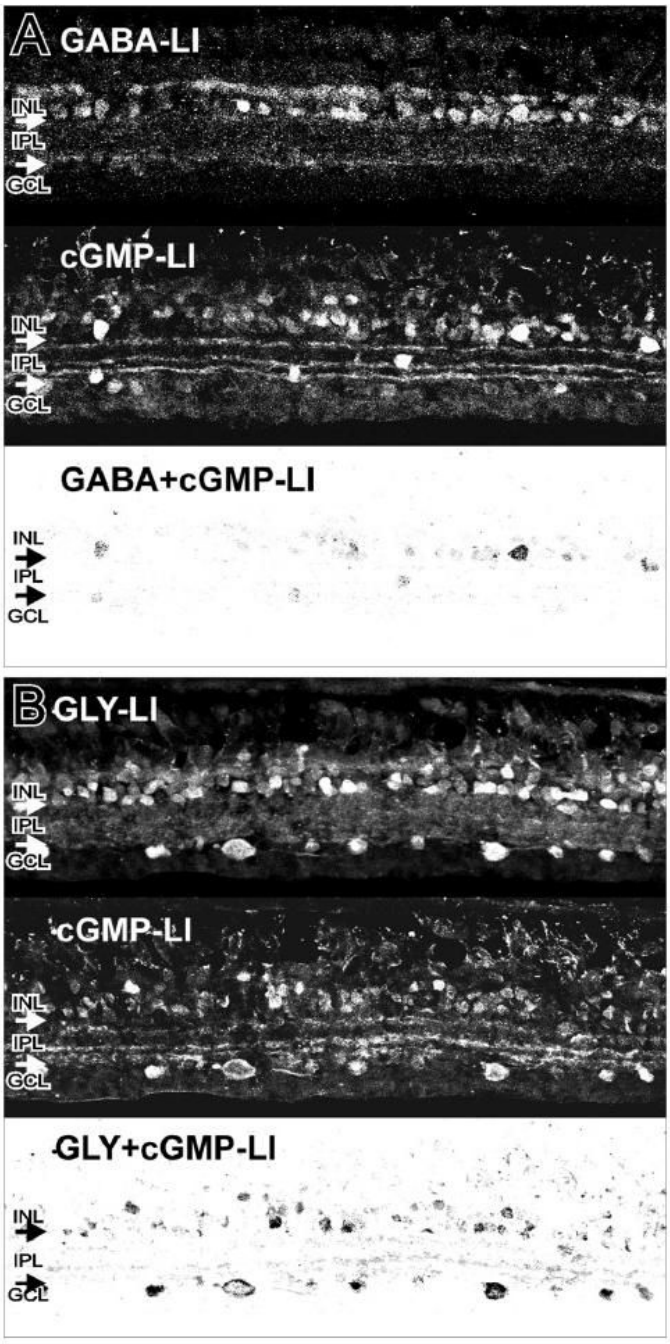

Fig. 5.

Colocalization of cGMP with GABA or GLY. A: The top panel shows strong GABA-LI in select amacrine cell somata, and in synaptic boutons in the IPL. The middle panel shows strong cGMP-LI in a retina treated with NO donor. The bottom panel shows a contrast inverted image of the colocalization of GABA-LI and cGMP-LI in some amacrine cell somata and in some processes and synaptic boutons in the IPL. B: The top panel shows strong GLY-LI in amacrine cell somata, somata in the GCL, and in synaptic boutons in the IPL. The middle panel shows strong cGMP-LI in a retina treated with NO donor. The bottom panel shows a contrast inverted image of the colocalization of GLY-LI and cGMP-LI in numerous amacrine cell somata,

somata in the GCL, and in processes and synaptic boutons in the IPL. These data were the average of 30 images from 3 animals (10 per animal) for each antibody.

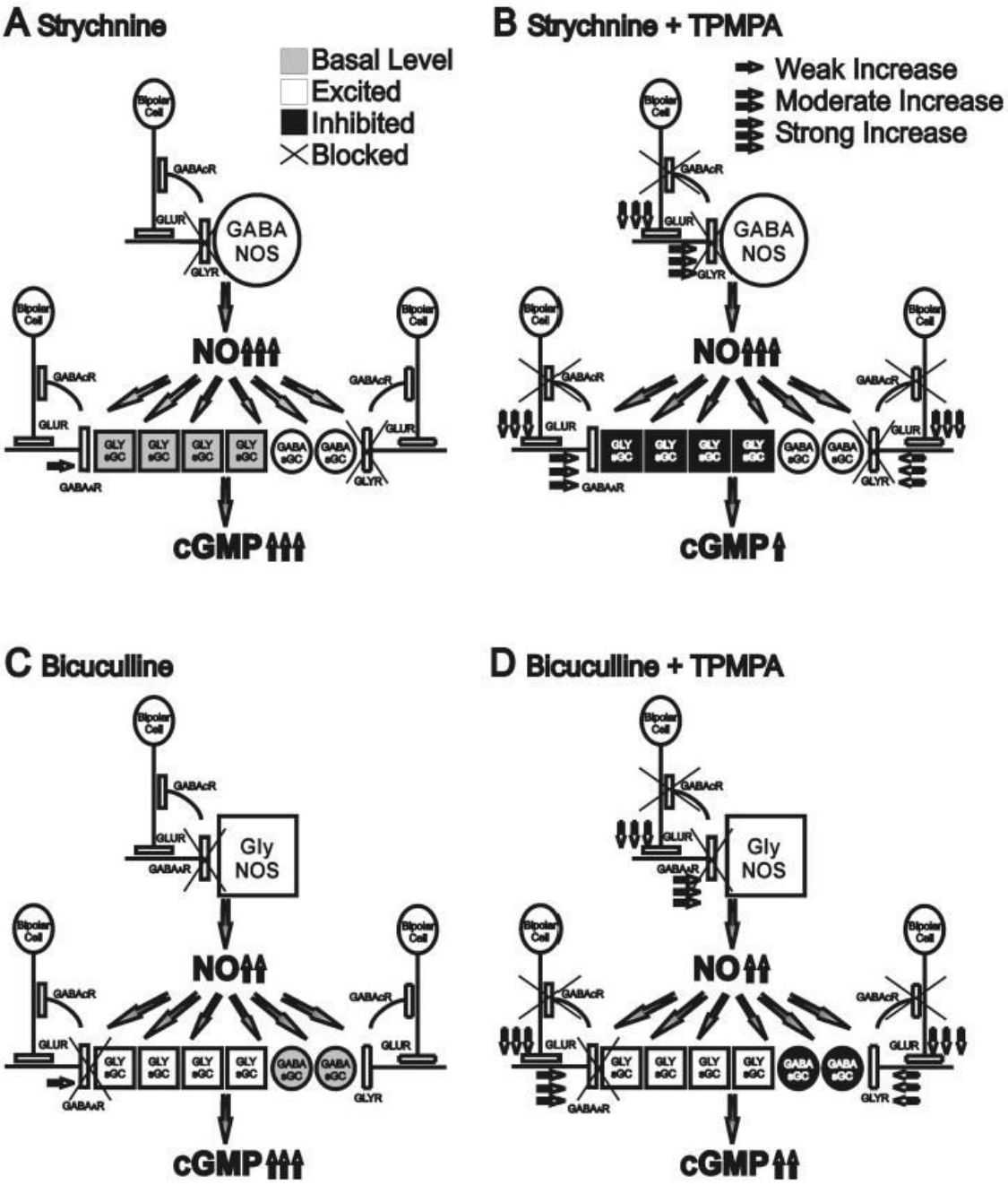

Fig. 6.

A: Strychnine treatment alone disinhibits GABAergic synaptic boutons that express NOS, leading to strong production of NO. GABAergic NOS amacrine cells may have wide-field arborizations and potentially more synaptic boutons expressing NOS than glycinergic amacrine synaptic boutons. These high levels of NO stimulate basal levels of sGC in glycinergic synaptic boutons still receiving $GABA_AR$ inhibition and activate sGC in disinhibited GABAergic synaptic boutons receiving glycinergic inhibition, leading to strong cGMP production. B: Adding TPMPA enhances glutamate output from the bipolar cell axon terminals onto both GABAergic and glycinergic amacrine dendritic processes, leading to enhanced inhibition between amacrine cells. However, the presence of strychnine prevents enhanced glycinergic

inhibition of GABAergic synaptic boutons containing NOS or sGC, therefore the level of NO production from GABAergic cells should remain similar to that seen with strychnine alone. Enhanced GABAergic inhibition through $GABA_AR$, however, would reduce the activity of sGC in glycinergic synaptic boutons. The net result of adding TPMPA would be similar levels of NO production but reduced cGMP production. It is also possible that the sources of NO are further away from the cells with sGC. C: Bicuculline treatment alone disinhibits glycinergic synaptic boutons expressing NOS. However, since glycinergic amacrine cells may be narrow-field cells, potentially having fewer synaptic boutons containing NOS, the effect of bicuculline on NO production is moderate. Since cGMP production is predominantly localized with glycine, more synaptic boutons expressing sGC may be glycinergic. Bicuculline would excite these glycinergic sGC-containing synaptic boutons, increasing the NO-sensitivity of the sGC in these boutons to the moderate levels of NO, still permitting a strong increase in cGMP levels. It is also possible that the sources of NO are closer to the cells with sGC. D: Adding TPMPA will enhance the glycinergic inhibition on the minority of sGC-containing synaptic boutons that are GABAergic, leading to slightly reduced cGMP levels.

Table 1

Comparisons of cGMP-LI and NO-IF in turtle retinasa

	cGMP-LI					
	Cell types		Regions			
Treatment	Amacrine	Bipolar	Superior	Central	Inferior	NO-IF
*BIC	sGC A1, sGC A2, sGC A3, sGC 4, sGC A5, sGC A11 somata in GCL	sGC B1, sGC B2, sGC B3.	+++ 1-2 bands	+++ 3 bands	++ 2 bands	++
STRY	sGC A1, sGC A2, sGC A3, sGC 4, sGC A11 (rare)	sGC B1, sGC B2,	++ 2 bands	+ 2 faint bands	++ 1-2 bands	+++
*BIC +TPMPA	sGC A1,	-	++	++	++	++
	sGC A2, sGC A3, sGC A5		1-2 bands	2 bands	2 bands	
STRY +TPMPA	sGC A1,	-	+	-	+	+++
	sGC A2, sGC A3		2 faint bands		1 faint band	
BIC+STRY	sGC A1, sGC A2, sGC A3, sGC 4, sGC A5, sGC A11 somata in GCL	sGC B1, sGC B2, sGC B3.	+++ 2 bands	+++ 3 bands	++ 2 bands	+++
BIC+STRY +TPMPA	sGC A1,	sGC B1,	++	+++	++	+++
	sGC A2, sGC A3, sGC 4, sGC A5, sGC A11 somata in GCL	sGC B2, sGC B3.	2 bands	3 bands	2 bands	

[a]Treated with 100 μM BIC, 100 μM STRY, 100 μM BIC + 100 μM TPMPA, 100 μM STRY + 100 μM TPMPA, 100 μM BIC + 100 μM STRY, or BIC +STRY+TPMPA (100 μM each). "*" indicates that the cGMP-LI data are from an earlier study (Yu & Eldred, 2005). "+++" indicates strong increase in cGMP-LI or NO-IF; "+" indicates slight increase in cGMP-LI or NO-IF;"++" indicates moderate increase in cGMP-LI or NO-IF. The number of cGMP-LI positive bands in the IPL is presented for each treatment in different retinal regions.